学位申請論文

今里哲久

THE MECHANISM OF THE DEVELOPMENT OF WIND-WAVE SPECTRA

By

Norihisa IMASATO

Abstract: The mechanism of the development of wind-waves will be proposed on the basis of the observed wave spectra in the wind tunnels and at Lake Biwa (IMASATO, 1976). It consists of two aspects: one is that the air flow over the wind-waves transfers momentum concentratively to the steepest component waves and the other is that the upper limit of the growth of a wave spectral density is given by the ultimate value in the slope spectral density. The first aspect means that the wave field has the "momentum transfer filter" on receiving the momentum from the air flow. Wind-waves in the stage of "sea-waves" receive the necessary amount of momentum by the form drag, e.g. according to the MILES' (1960) inviscid mechanism, through a very narrow frequency region around a dominant spectral peak. On the other hand, wind-waves in the stage of "initial-wavelets" receive it according to the MILES' (1962a) viscous model through a fairly broad frequency region around the peak. The upper limit of S_{max} developing according to viscous mechanism is given by $S_{max}=6.40\times10^{-4}K_{max}^{-2}$ $cm^2\cdot sec$ and $S_{max}=2.03C(f_{max})^{-2}$ $cm^2\cdot sec$ (S_{max} is the power density of the wave spectral peak with the frequency f_{max}, K_{max} is the wave number corresponding to the frequency f_{max} and C is the phase velocity).

From the second aspect, the upper limit of the growth of wave spectral density is given by $33.3f^{-4}$ $cm^2 \cdot sec$ in the frequency region of late stage of "sea-waves". Therefore, the spectral peak, which has the largest value in the slope spectral density in the component waves of the wave spectrum, rises high over the line $4.15f^{-5}$ $cm^2 \cdot sec$. The energy is transported from the spectral peak to the high frequency part and to the forward face of a wave spectrum by nonlinear wave-wave interaction. This nonlinearity is confirmed by the bispectra calculated from the observed wind-wave data. In the stage of "sea-waves", nonlinear rearrangement of the wave energy comes from a narrow "momentu transfer filter", and, in the stage of "initial-wavelets", it comes mai from small corrugations and small steepness of the wave field.

1. Introduction.

A large number of informations on wind-waves in wind tunnels and at oceans have been accumulated, but the mechanism of momentum transfer to wind-waves or of the development of wind-waves seems to be mysterious. JEFFREYS (1924) studied this problem by considering the pressure fluctuation in phase with the wave slope and the shelterir effect. BENJAMIN (1960) and MILES (1962a) examined theoretically a development of small scale wind-waves at the early stage, and pointed out a possibility of wave growth by the viscous Reynolds stress in the laminar sub-layer in the immediate neighbourhood of the water surface. MILES (1960) showed that the PHILLIPS' (1957) resonance mechanism explains the generation and the development of a wind-wave spectrum at

the early stage, and that the MILES' (1957, 1959, 1960) inviscid model explains the late stage of the development. LIGHTHILL (1962) made clear the physical meaning of the MILES' inviscid model, and the problem of the development of wind-wave spectrum seemed to be solved by their studies. However, SNYDER and COX (1966) found out that the amplification coefficient β, expected from the MILES' theory, can not explain the development of the wind-waves at open oceans. BARNETT and WILKERSON (1967) and others supported the result of SNYDER and COX.

Some investigators have tried to attribute this discrepansy between the linear theories and the observed results to the turbulence in the air flow over the wind-waves (YEFIMOV, 1970; REYNOLDS and HUSSAIN, 1972; FUJINAWA, 1974). And also, many trials to clarify the structure of the air flow over a wavy water surface as well as the mechanism of momentum transfer from the air flow to wind-waves have been made by PHILLIPS (1966), SHEMDIN and HSU (1967), DOBSON (1971), DAVIS (1972), ICHIKAWA and IMASATO (1976) and others.

Nevertheless, we have obtained only a few knowledge about these problems, and when we adopt the turbulent model on the momentum transfer to the wind-waves, we must introduce some important assumptions on the structure of the turbulent wind (ICHIKAWA and IMASATO, 1976)

On the other hand, in order to explain the actual development of a wind-wave spectrum, the mechanisms of rearrangement of the wave energy in a wave spectrum, such as the wave-wave interaction (KINSMAN,

1965; BARNETT, 1968; HASSELMANN et al., 1973), overshoot phenomena (BARNETT and WILKERSON, 1967; BARNETT and SUTHERLAND, 1968; MITSUYASU, 1968), and so on, have been studied by many investigators. HASSELMANN et al. (1963), NAGATA (1970), and KAKINUMA et al. (1968) showed that the bispectrum analysis is very useful in order to get informations on a nonlinearity of a wave field. IMASATO (1976) discussed some interesting characteristics of the development process of wind-waves and showed that the development process of wind-waves is classified in the similar way to KUNISHI's (1963) classification in three stages: "sea-waves", "transition stage" and "initial-wavelets". They are summarized in Fig. 1, using the spectral density S_{max} of the wave spectral peak. This figure is the same as Fig. 5 in the author's previous paper (IMASATO, 1976). In the present paper, a mechanism on development of the wind-wave spectrum is proposed on the basis of the results reported by IMASATO (1976). It consists of two aspects; one is that the air flow transfers the momentum concentratively to the steepest component waves; i.e. the wave field has the "momentum transfer filter on receiving the momentum from the wind, and the other is that the upper limit of the growth of the wave spectral density is given by the ultimate value in slope spectral density. In the late stage of the "sea-waves", this upper limit is given by $33.3f^{-4}$ $cm^2 \cdot sec$ shown in Fig. 1, where the broken curves indicate the wave spectrum S(f) which is given as

$$S(f) = \alpha_1 k^{-2} \qquad (1)$$

where α_1 is a constant value in slope spectral density. In conclusion, we suggest that the concentrative momentum transfer from the wind to the steepest component wave must be considered instead of the momentum transfer according to the linear models, and that the nonlinear wave-wave interaction and the slope spectral density are important and essential factors in the development of wind-waves.

2 Momentum transfer from the air flow to wind-waves.

If wind-waves dissipate energy due only to the kinematic viscosity of water ν_w, the energy equation for a component wave of the frequency f is given as follows,

$$\frac{\rho_w g}{2}\left[\frac{\partial S(f)}{\partial t} + \frac{\partial}{\partial x}C_g(f)\cdot S(f)\right] = R_N(f) - 2\rho_w\nu_w g k^2 S(f) + R_{NON}, \quad (2)$$

where ρ_w is the density of water, g the acceleration of gravity, t time, $C_g(f)$ the group velocity of the wave of the frequency f, $R_N(f)$ the energy flux to the wind-wave, R_{NON} the energy flux by the wave-wave interaction, and the x-axis is chosen for the direction of wave propagation. In the field observations, the second term of the left side of Eq. 2 is assumed to be negligible, and, on the other hand, the first term is just equal to zero in the wind tunnel experiments. Therefore, effective momentum flux $\tau_w(f)$ is given by Eq. 3 in the case of the field observations,

$$\tau_w(f) = \frac{\rho_w g}{2} \left[\frac{\partial}{\partial t} \cdot \frac{S(f)}{C(f)} + 4\nu_w k^2 \cdot \frac{S(f)}{C(f)} \right] + \tau_{NON}, \qquad (3)$$

where τ_{NON} is the momentum flux by the nonlinear wave-wave interaction, and by Eq. 4 in the case of the wind tunnel experiments,

$$\tau_w(f) = \frac{\rho_w g}{2} \cdot \left[\frac{1}{2} \cdot \frac{\partial S(f)}{\partial x} + 4\nu_w k^2 \cdot \frac{S(f)}{C(f)} \right] + \tau_{NON}. \qquad (4)$$

$\tau_w(f)$ indicates the least amount of momentum flux which the wind-wave spectrum of the frequency f needs to develop from $S_1(f)$ to $S_2(f)$ as shown in Fig. 2. This figure is the schematic diagram which shows the growth of wind-waves in the two stages: (a) is for "sea-waves" and (b) for "initial-wavelets". The chain curves indicate the power spectral density $S(f) = \alpha_1 k^{-2}$ shown by the broken curves in Fig. 1. S(f) of the second term in the right side of Eq. (3) or Eq. (4) is given by $S_0(f)$ which is estimated from $S_1(f)$ and $S_2(f)$ as shown in Fig. 2.

Two examples of the spectrum $\tau_w(f)$ are shown by the solid curves in Fig. 3; (a) shows the spectrum of Run-19 and (b) that of Run-12, and they are evaluated at the fetch 12.4m (the middle point between fetches 9.7 and 15.1m). The former is an example of the spectrum in the stage of "sea-waves" and the part of spectral density, shown by the broken curve, indicates the absolute value of the spectral density. The latter is an example of the spectrum in the stage of "initial-wavelets". In this paper, definitions on Run numbers and the stages

of development of wind-waves are the same as those in the previous paper of the author (IMASATO, 1976). Arrows in the figure indicate the frequency f_{max} of the wind-wave spectral peaks.

We define the effective momentum flux τ_{ws} transferred from the air flow to the wave field as follows,

$$\tau_{ws} = \int_0^\infty J \cdot \tau_w(f) \cdot df, \tag{5}$$

where J is given as

$$J = \begin{cases} 1, & \text{when} \quad \tau_w(f) \geq 0, \quad (6\text{-}1) \\ 0, & \text{when} \quad \tau_w(f) < 0. \quad (6\text{-}2) \end{cases}$$

The integral of the nonlinear term τ_{NON} with respect to the frequency in Eq. (5) vanishes, and therefore, only two terms in the bracket in the right side of Eq.(3) or Eq.(4) may be evaluated in estimation of τ_{ws}. τ_{ws} indicates the necessary amount of momentum for a wind-wave spectrum to develop from S_1 to S_2 which are schematically shown in Fig. 2.

We must evaluate the momentum flux $\tau_M(f)$ from the wind to the wind-waves. We consider that the momentum is transfered according to the form drag. Until SNYDER and COX (1966) found out that the MILES' coefficient β of the wave amplification was too small to explain the growth of wind-waves at open oceans, the MILES' (1957, 1960) inviscid model had been considered to be the most successful

model to explain the development of wind-wave spectra. But the actual wind-field over wind-waves is not inviscid but turbulent. Therefore, we must numerically solve the viscous Orr-Sommerfeld equation to evaluate the momentum flux from the turbulent wind to the wind-waves. But, unfortunately, we must introduce some important assumptions on the boundary condition and the structure of the turbulent wind (YEFIMOV, 1970; REYNOLDS and HUSSAIN, 1972, and ICHIKAWA and IMASATO, 1976). Therefore, it is very doubtful for our present problem whether the numerical viscous solution is superior to the MILES' solution which has been discussed by many investigators. Therefore, we will advance the discussion, adopting the MILES' inviscid mechanism.

A spectral density $\tau_M(f)$ of momentum flux from the air flow to the component wave of the frequency f is written after MILES (1957) as follows:

$$\tau_M(f) = \rho_a \left(\frac{u_*}{\kappa}\right)^2 \beta(f) k^2 S_0(f), \tag{7}$$

where ρ_a is the density of air, κ the KARMANN's constant, and $S_0(f)$ the wind-wave spectral density estimated from $S_1(f)$ and $S_2(f)$ as shown in Fig. 2. The coefficient $\beta(f)$ is calculated graphically from the MILES' (1960) numerical result. Two examples of the frequency spectrum $\tau_M(f)$ from the wind tunnel experiment are shown by the dotted curves in Fig. 3 together with the spectra $\tau_w(f)$; (a) is the spectra of Run-19 and (b) those of Run-12 at the fetch 12.4m. It must be mentioned that τ_{NON} is excluded from $\tau_w(f)$ in Fig.3.

3. Mechanism of the growth of the "sea-waves".

Fig. 3(a) clearly shows that the spectrum $\tau_M(f)$ has a dominant peak at the frequency f_{max} in the spectral peak in the wind-wave spectrum, and that the relation $\tau_M(f)<\tau_w(f)$ is found in the forward face of the wave spectrum in the stage of sea-waves. It indicates that the MILES' coefficient β or the MILES' inviscid model can not explain the growth of the forward face of the wind-wave spectra calculated from the wave data in the stage of "sea-waves" if we consider that each component wave of the wave spectrum receives momentum by the normal pressure fluctuations of the same frequency, i.e., we consider the linear model.

We define the quantity τ_{MS} as follows:

$$\tau_{MS} = \int_{f_{max}-\delta f_1}^{f_{max}+\delta f_2} \tau_M(f)\cdot df\cdot \qquad (8)$$

We define δf as $\delta f_1+\delta f_2$, and define f_R as a significant frequency band width in the wind-wave spectrum. In the actual procedure in the evaluation of τ_{MS}, δf_1 and δf_2 are chosen as $\tau_M(f_{max}-\delta f_1) = \tau_M(f_{max}+\delta f_2)$. The wind-wave spectrum in the stage of "sea-waves" has the frequency region δf ($<f_R$) giving the relation $\tau_{ws}=\tau_{MS}$. In the case of Run-19 (Fig. 3(a)), δf is 0.257 and $\delta f/f_R$ is 0.0228. Values of δf and $\delta f/f_R$ from the wind tunnel experiments and the field observations are summarized in Table 1. These results indicate that, even though the linear model can not explain the growth of the

forward face of an observed wind-wave spectrum, the MILES' inviscid mechanism can explain the supplement of the greater amount of momentum than the whole amount that the wind-wave field requires, i.e. we have the relation $\tau_{MS} > \tau_{ws}$. In consideration of these situations, we propose the following model on the momentum transfer from the wind to the "sea-waves". The steepest component waves, which make the dominant peak in the power spectrum of the "sea-waves", receive the almost whole amount of momentum necessary for wind-waves to develop. And then, they nonlinearly transport the momentum to the forward face of the spectrum in order to rise the energy level and to the higher frequency part in order to compensate energy loss due to viscosity.

We understand this concentrative transfer of the momentum from the wind as follows: Momentum flux to wind-waves is generally given by the mean product of water surface slope $\partial\eta/\partial x$ and pressure fluctuation p. Therefore, the spectrum of the momentum flux in the present model is proportional to the slope spectrum $\phi(f)$, and it has a dominant peak at the frequency where the slope spectral density is largest. After IMASATO (1976), the component waves around a wave spectral peak in the stage of "sea-waves" have the largest value in a slope spectral density, and that the value in the slope spectral density of the high frequency part in the wind-wave spectrum is not constant but decreasing with the frequency. Therefore, when a wind-wave field has a broad band spectrum, the component waves around the wave spectral peak contribute most largely to steepness

of the wave field and also to the corrugation of the water surface. They will also contribute most greatly to the pressure fluctuation p of the wind field undulated by the water surface corrugation. It means that MILES' coefficient $\beta(f_0)$ for any component wave of the frequency f_0 far from the frequency f_{max} of the wave spectral peak will be reduced to be very small in comparison with the coefficient in the case where the wave field consists of the single component wave of the frequency f_0. Therefore, in the case of "sea-waves", most amounts of momentum are transferred to the wave field through the wave spectral peak, and component waves in the high frequency part and those in the forward face of wave spectrum will receive the less amount of momentum from the wind than that expected from the linear theory.

About this phenomenon, it is convenient for us to understand that the wind-wave field has a kind of filtering effect on the momentum transfer from the wind to wind-waves. We call this filter the "momentum transfer filter" in this article. The fact that $\delta f/f_R$ in Table 1(a) becomes smaller as the wind-waves develop indicates that the width of this filter becomes narrower as the wind-waves develop.

It must be noticed that the values of δf in the four cases marked with a plus sign in Table 1 must be treated as the results of formal application of the present procedure, because, in these cases, wind-waves break by the strong wind and τ_M must be evaluated according to any other mechanism.

The calculated spectrum of $\tau_M(f)$ in Fig. 3 or Fig. 4(a) (dotted curves) does not pass through this "momentum transfer filter" The actual spectrum of $\tau_M(f)$ should pass through the filter and will have a dominant peak at the frequency f_{max}. The spectrum $\tau_M(f)$ in the present model will be expressed by the chain curve in Fig. 4(a). However, actually, the wave field will not have such a sharp filter, and the actual spectral form of $\tau_M(f)$ should be shown by the solid curve in Fig. 4(a), although it could not be quantitatively evaluated in this article. After all, we can conclude that $\tau_M(f_{max})$ contributes most largely to τ_{MS} in the case of the "sea-waves".

4. Mechanism of the growth of "initial-wavelets".

The results shown in Table 1(a) and Fig. 3(b) indicate that the MILES' inviscid mechanism can not explain the necessary amount of momentum transferred from the air flow to the "initial-wavelets". Therefore, any other mechanism must be considered on the momentum transfer from the air flow to the "initial-wavelets"

PHILLIPS' (1957) resonance mechanism could not be effective in this case, because the values of $2m_I(f)F_0/C_g(f)$ calculated from the present data are larger than unity in the frequency range f_R ($m_I(f)$ is the growth factor spectrum according to MILES' inviscid model). Vertical profile of turbulent wind at the outside of the laminar sub-layer over wind-waves is usually expressed as

$$\frac{u}{u_*} = 5.75 \cdot \log \frac{z}{z_0} ,$$

$$= 5.75 \cdot \log \frac{u_* Z}{\nu_a} - 5.75 \cdot \log \frac{u_* Z_0}{\nu_a}$$

$$= 5.75 \cdot \log \frac{u_* Z}{\nu_a} + E. \qquad (9)$$

If the wind-waves have the same characteristics as the solid wall in a pipe, there exists a laminar sub-layer when E=5.5 (SCHLICHTING, 1955) As the wind-waves develop, the value of E becomes smaller and the water surface becomes completely rough (KUNISHI, 1963). It is not clear unfortunately whether the laminar sub-layer exists in this condition E<5.5. Then, we assume that the laminar sub-layer exists if two curves of Eq. 9 and $\frac{u}{u_*} = \frac{u_* Z}{\nu_a}$ intersect each other. Therefore, according to this assumption, we get

$$0.20 \leq E \leq 5.5 \qquad (10)$$

as the condition of existence of the laminar sub-layer. Values of E for the five cases in the stage of "initial-wavelets", where the MILES' inviscid model can not be effective, are tabulated in Table 2. It is shown from this table that the laminar sub-layer exists in these five cases

In this situation, resonance between the Tollmien-Schlichting wave in the laminar sub-layer and the "initial-wavelets" (BENJAMIN, 1960; MILES, 1962a) may explain the development of the "initial-wavelets" But this resonance occurs at the low frequency range too far from the lowest frequency in the significant frequency range of the wave spectrum of "initial-wavelets" in the present data

(Table 3)

Next, we consider the momentum flux transferred by the viscous Reynolds stress, which was discussed by BENJAMIN (1959) and MILES (1962a) MILES' (1962a) result gives the growth factor $m_v(f)$ for a wave of the frequency f as

$$m_v = \frac{su_*^2}{2\nu_a} \left[\frac{\mathcal{W}_i - \mathcal{F}_i - (\nu_a k/u_*)^{2/3}(\mathcal{W}_r - \mathcal{F}_r)\mathcal{H}_i}{|\mathcal{F} - \mathcal{W}|^2}\right]_{C=C_0}, \qquad (11)$$

where s is ρ_a/ρ_w, C_0 is $(g/k+\sigma k)^{1/2}$ and σ is surface tension of water. The suffixes i and r indicate the imaginary and the real parts of complex variables, respectively. The other parameters $\mathcal{F}_i$, $\mathcal{F}_r$, $\mathcal{H}_i$ and $\mathcal{W}_r$ are given graphically in MILES (1962b) And the parameter $\mathcal{W}_i$ is put to equal zero, because the wind profile is assumed to be linear The growth factor $m_v(f)$, given by Eq. 8, is effective for the waves with a phase velocity less than the wind speed at the edge of the linear wind profile, which is put to equal $5u_*$. The spectrum $\tau_M(f)$ of the momentum flux from the air flow with the linear profile is given as

$$\tau_M(f) = 2m_v(f) \cdot k \cdot C_0(f) \cdot S(f) \qquad (12)$$

Two calculated spectra $\tau_M(f)$ and $\tau_W(f)$ at F=12.4m are shown in the upper part of Fig. 5; (a) is for Run-11 and (b) for Run-12. $\tau_W(f)$ is plotted by the solid curve and $\tau_M(f)$ by the dotted curve. Using these spectra $\tau_M(f)$ and $\tau_W(f)$, we evaluate $\delta f/f_R$ to be 0.38 $\sim$0.53 (Table 2) It indicates that the wave field of "initial-wavelets" has a "momentum transfer filter" similar to the filter of the wave field of "sea-waves" However, δf in this stage is broader than that in the stage of "sea-waves" It is attributed to the small corrugations and the small steepness of the wave field. The spectrum $\tau_M(f)$ given by the MILES' viscous model is shown in Fig 4(b) by the dotted curve, and the spectrum $\tau_M(f)$ given after passing through the momentum transfer filter" is shown by the chain curve.

In the lower part of Fig. 5, the spectra of $m_v(f)$ according to the viscous model are plotted by the dotted curves and the spectra of the net growth factor $m(f)=m_v(f)-2k^2\nu_W$ are also plotted by the solid curves For reference, the spectra of the growth factor $m_I(f)$ are plotted in this figure by the broken curves on the assumption of a logarithmic wind profile. We can clearly find out that $m_v(f)$ is much larger than $m_I(f)$ in whole frequency range of the wave spectrum, especially in the frequency range from 5Hz to about 8Hz.

Fig 6 shows the schematic spectra of $\tau_M(f)$, S(f), and the wave spectrum given by Eq. 1. The frequency range δf corresponds to the frequency range $S(f)>\alpha_1 k^{-2}$ (chain curve) It means that the momentum is transferred to the "initial-wavelets" through the frequency region with the large slope spectral densities. The wave spectrum of "initial-

wavelets" has a fairly broad frequency region (IMASATO, 1976), giving the constant value in the slope spectral density, which is the ultimate value in this wave spectrum. This frequency region is at the higher frequency part than the frequency f_{max} in the wave spectral peak, and it corresponds to the frequency region, giving the net growth factor m(f) of a large value. The spectrum $\tau_M(f)$ of the momentum flux has a peak at the frequency with the maximum value Φ_{max} in the slope spectral density, and a new dominant wave spectral peak is made at this frequency. Therefore, the spectral peak moves to the higher frequency as the wind-waves develop.

There is another reason why a wave spectral peak moves to the higher frequency. The wave field of "initial-wavelets" has a very small wave height and a very small steepness. And in order that this wave field can effectively receive the momentum from the air flow, the wave field of "initial-wavelets" must become as steep as possible and also many component waves must become steeper with a little amount of momentum flux. The wave field will succeed this trial if a component wave, e.g., the wave spectral peak of the wave spectrum S_1 in Fig 7, transports nonlinearly large amount of momentum to the other component waves of the higher frequency. If the component wave develops along the line 1, as schematically shown in Fig. 7, which crosses perpendicularly to a wave spectrum $\alpha_1 k^{-2}$ with a constant value α_1 in the slope spectral density, the same case happens. From these reasons, the wave spectrum of 'initial-wavelets' has the broad frequency region of the constant value in the slope spectral

density. Of course, if the wave spectral peak develops to S_3 along the line 3, the wave field will have the same slope spectral density α_1, although in this case several times of momentum must be transferred from the air flow to the waves. Actually, the large amount of momentum transferred to the waves will be used for the latter development process. As the result, the wave spectrum S_1 will develop along the line 2 to the spectrum S_2 and the wave spectral peak moves to the higher frequency.

In the high frequency range, for example in larger frequencies than 8Hz in Run-11 in Fig. 5, the relation $\tau_w(f) > \tau_M(f)$ is found, and, therefore, the net growth factor m(f) is negative because of a great amount of wave energy dissipation due to the viscosity. Nevertheless, the observed wave spectral densities at those frequency ranges develop larger. It indicates that the wave energy is nonlinearly transported from the wave spectral peak to those high frequency components of the wave spectrum. Therefore, the nonlinear wave-wave interaction is also one of the important and fundamental characters in the development of the wind-wave spectrum.

We find out that the development of "initial-wavelets" can be explained by the MILES' viscous model on the assumption of the momentum transfer filter and of the nonlinear wave-wave interaction. Using the spectral density $S(f_{max})$, we will define the region where the wind-waves develop according to the viscous model. Conditions that the critical heights Zc for a component wave propagating with the phase velocity C is always within the laminar sub-layer are given by the following equations,

$$E = 0.20 \text{ or } \frac{u_* z_0}{\nu_a} = 0.923, \qquad (13\text{-}1)$$

and

$$\frac{u_* z_c}{\nu_a} \leq 2.4 \text{ or } \frac{C}{u_*} \leq 2.4. \qquad (13\text{-}2)$$

After KUNISHI (1963), wind-waves in a wind tunnel are similar in characteristics to the roughness of the solid wall in a pipe and he proposed Eq. 14 as the relation between the roughness height h (he took h as the mean wave heights) and the roughness parameter z_0,

$$\frac{u_* h}{\nu_a} = 10\left(\frac{u_* z_0}{\nu_a} - \frac{1}{9}\right). \qquad (14)$$

If we assume the roughness height can be expressed by $2\sqrt{S(f_{max})df}$, the wave spectral density of the peak must be smaller than $2.03C(f_{max})^{-2}$ according to Eqs. 13 and 14. The relation $S(f_{max})=2.03C(f_{max})^{-2}$ is shown in Fig. 1 by the thick dotted curve. Considering the results shown in Fig. 1, wave spectral density developed according to the MILES' viscous mechanism must be smaller than that given by $2.03C(f_{max})^{-2}$

According to IMASATO (1976), transition from the "initial-wavelets" to the "transition stage" is given by $S_{max}=6.40\times10^{-4}K^{-2}$ This relation corresponds to the condition whether the viscous mechanism can be available. This condition also indicates that the "initial-wavelets" become so steep and large that the air flow becomes completely rough and the laminar sub-layer diminishes.

5. Upper limit of the growth of the wave spectral density and non-linear wave-wave interaction.

We explained the development process of wind-wave spectra using the momentum transfer filter and the MILES' mechanism (MILES, 1960, 1962a) There are some problems to be discussed in order to accept the present mechanism on the momentum transfer to wind-waves. The first is: What is the physical meaning of the f^{-5} law which many wave spectra obtained from the field observations follow? The second is: What prepares the upper limit of the growth of a wave spectral density? The third is: Whether nonlinear wave-wave interaction, assumed in this article, can be proved in observed wave spectra.

(5-1). The f^{-5} law and the upper limit of the growth of wave spectra.

The results of the field observations at Lake Biwa show that a wave spectral peak develops along the line $4.15f^{-5}$ and the high frequency part in a wave spectrum, obtained in an increasing wind velocity, lies on this f^{-5} line. The f^{-5} law has been considered to be maintained by breaking of very steep component waves of the high frequency part in the wave spectrum (PHILLIPS, 1958). If this concept is true, the present results must indicate that the component wave of a wave spectral peak is breaking, because the component wave of the spectral peak is steepest in the wave spectrum (IMASATO, 1976). The wave spectral peaks obtained from the experiment Ex-KI, where the breaking by a strong wind occurs, rise high from the line $4.15f^{-5}$ and the high frequency part in the wave spectrum does not follow the f^{-5} law. The overshoot phenomena of wave spectral peaks

have been known to occur frequently not only in wind tunnels but also at oceans. We also obtained such an example from the observations at Lake Biwa (IMASATO, 1976). Therefore, it may be concluded that the f^{-5} law does not present the upper limit of the growth of the component wave of the wind-wave spectrum.

We can suppose that the upper limit of the development of any component wave is given by the ultimate value in a slope spectral density. It is analogous to the classical concept that a wind-wave can grow until its steepness becomes maximum. According to IMASATO (1976), this upper limit of the wave spectral density is given by $33.3f^{-4}$ ($cm^2 \cdot sec$) in the gravity wave region.

If a component wave of a wave spectrum develops along the line f^{-5}, the slope spectral density of this component wave increases with the development and is not constant. Therefore, the f^{-5} law is not maintained by breaking of the steep waves in the high frequency part in the wave spectrum. If the equilibrium state is maintained by breaking of the waves with the maximum value in the slope spectral density, the wave spectral density in this stage should be proportional to f^{-4}

In the case of the wind tunnel experiments, wind continues to blow uniformly over the wavy water surface and the "tight"* coupling between the shear flow and the water surface corrugations will be expected. On the other hand, the wind field at oceans has a spatial

---

* Of course, the word "tight" is used in a relative sence, and does not mean the strong coupling such as breaking of waves.

distribution and a time variation, and the wave field is very complex due to the directional dispersion of energy and so on. The coupling between the shear flow and the wind-waves at oceans may be weaker than that in the wind tunnels. The wave spectral peaks in the stage of "sea-waves" develop along the line $4.15f^{-5}$ at the increasing wind velocity, and those in an attenuating wind or those of swells coming from the off-shore, is situated far below the line $4.15f^{-5}$, although they are not shown in any figure. From these facts, we can consider that the $4.15f^{-5}$ line prepares the lower limit of the spectral density S_{max} in the wave spectral peak in the state of the local energy balance with the developing wind field and in the state of developing by the form drag. If the wind continues to blow uniformly over the water surface at oceans as in the wind tunnels, the "tight" interaction will be expected and as the result, the spectral peak will rise high from the line $4.15f^{-5}$. Therefore, the overshoot phenomenon of a wave spectrum is one of the natural and fundamental features of the development process of the wind-wave spectrum. The envelope of the wave spectral peaks from the wind tunnel experiments (Fig 1) will prepare the upper limit of the wave spectral density.

(5-2). Nonlinear wave-wave interaction.

The nonlinearity of wind-waves is mainly attributed to the fact that the wave field has the narrow filter on the momentum transfer from the air flow. However, there are some other causes for the nonlinearity of the wind-wave field.

In the case of wind-waves in the stage of "sea-waves" or "transition stage", one of the causes of nonlinearity is that the observed spectrum $\tau_w(f)$ has a frequency region of negative spectral density, or in another word, the wind-wave spectrum has an overshooting spectral peak. In Fig 3(a), the absolute value of negative value of spectral density $\tau_w(f)$ of "sea-waves" is shown by the mark ⊷ and broken curve. This negative part comes from the shaded part of the wave spectrum of "sea-waves" in Fig. 2(a) A part of the wave energy of this negative part will be transported to the forward face of the wave spectrum in order to rise its energy level, and another part will be transported to the high frequency part of the wave spectrum in order to compensate the energy loss due to the viscosity, and the rest will be used to produce the turbulence in water.

On the other hand, $\tau_w(f)$ is positive over the whole frequency band in a wave spectrum in the stage of "initial-wavelets". Nevertheless, nonlinearity in the "initial-wavelets" comes exactly from the fact that the spectrum $\tau_w(f)$ has no negative part. The spectrum of net growth factor m(f) for the "initial-wavelets" has a negative value at the high frequency range as shown in Fig. 5. Therefore, if the "initial-wavelets" have no nonlinear energy transport among the component waves in the wave spectrum, the wave spectral density in the frequency range with the negative net growth factor m(f) must be diminishing with the fetch. However, it has been found that an observed wave spectral density grows with fetch, and it must be attributed to the nonlinear energy transport from the component wave with

the largest slope spectral density to the higher frequency region in the wave spectrum. We have already mentioned in the Section 4 that the following two facts can be explained by the nonlinear wave-wave interaction; i.e., the wave spectral peak of "initial-wavelets" develops toward the higher frequency region and the wave spectrum of the "initial-wavelets" has a broad frequency region with a constant slope spectral density.

We must clarify from the data analysis whether there is a nonlinear wave-wave interaction among the wave spectral peak and the other component waves as assumed in this article. It was pointed out by TUKEY (1963), HASSELMANN et al. (1963), KAKINUMA et al. (1968), and NAGATA (1970) that the concept of a bispectrum is useful in studying the spectral characteristics of the non-Gaussian time series, i.e., the bispectrum of wave field brings us an information about a spectral structure of nonlinearity of the wind-wave field. Therefore, we calculated some bispectra using our wave data in order to make qualitative proof of our assumption on the nonlinear wave-wave interaction. Numerical calculation of the bispectrum $B(f_1, f_2)$ was performed by the method of KAKINUMA et al. (1968).

Fig. 8 shows some calculated bispectra; (a) is the bispectrum of wind-waves from the observations at Lake Biwa, and (b) and (c) are the bispectra from the wind tunnel experiments. Shaded parts in the figure indicate the frequency domains with the bispectral densities larger than 20% of the bispectral density B_{max} in a dominant bispectral peak. The dotted curves show the contour of the positive bispectral density

of $0.1B_{max}$, and the broken curves show the contour of the negative bispectral density of $-0.1B_{max}$. Wave (power) spectra are also plotted along two frequency axes, and the frequency regions of the wave spectrum with a constant slope spectral density are also shown by the thick solid curves.

The bispectrum (Fig. 8(a)) obtained from the field observations at Lake Biwa shows the nonlinear interaction between the wave spectral peak and the forward face of the wave spectrum, giving the positive bispectral density Fig. 8(b) is obtained from the experiment Ex-K. This bispectrum, calculated from the wave data in the stage of "sea-waves", shows the fairly simple features in comparison with the bispectrum from the field observations It proves more clearly the nonlinear interaction among the wave spectral peak and the higher and lower frequency parts of the wave spectrum. The bispectrum in Fig. 8(c) is calculated from the wave data of "initial-wavelets". It has more complicated features than the bispectra of "sea-waves", but it clearly shows the nonlinear interaction among the wave spectral peaks and the component waves with the higher and lower frequencies It must be emphasized that the nonlinearity spreads in the marvelously wide frequency areas. Those bispectra in Fig 8 support our present assumption on the nonlinear wave-wave interaction which occurs between the wave spectral peak and the forward face and high frequency part of the wave spectrum.

Based on the results presented above, it is concluded that nonlinear energy transport may be one of the essential factors in the

development of wind-waves. It is attributed to the "momentum transfer filter" and the large slope spectral density in the stage of "sea-waves", and is also attributed to the small wave height and the small steepness of the wave field in the stage of "initial-wavelets".

Acknowledgements

The author wishes to express his thanks to Professor H.KUNISHI of Kyoto University for his continuing guidance and encouragement. His thanks are also due to Mrs. Y.KIKUCHI for her assistance in the data processing. The calculations in this paper were carried out on FACOM 230-75 in the Data Processing Center of Kyoto University. A part of this study was supported by scientific research fund from the Ministry of Education.

REFERENCES

BARNETT,T.P. and J.C.WILKERSON (1967): On the generation of ocean waves as inferred from the airborne radar measurements of fetch-limited spectra, J. Marine Res , 25, 292-328.

BARNETT,T.P. and A.J.SUTHERLAND (1968): A note on an overshoot effect in wind-generated waves, J. Geophys. Res., 73, 6879-6885.

BARNETT,T.P. (1968): On the generation, dissipation, and prediction of ocean wind waves, J. Geophys. Res., 73, 513-529.

BENJAMIN,T.B. (1959): Shearing flow over a wavy boundary, J. Fluid Mech., 6, 161-205.

BENJAMIN,T.B. (1960): Effects of a flexible boundary on hydrodynamic stability, J. Fluid Mech., 9, 513-532.

DAVIS,R.E. (1972): On prediction of the turbulent flow over a wavy boundary, J. Fluid Mech., 52, 287-306.

DOBSON,F.W. (1971): Measurements of atmospheric pressure on wind-generated sea waves, J. Fluid Mech., 48, 91-127.

HASSELMANN,K., W.MUNK and G.MACDONALD (1963): Bispectra of ocean waves, Proc. Symposium on Time Series Analysis, John Wieley and Sons, Inc., 125-139.

FUJINAWA,Y. (1974): A model on the mechanism of momentum transfer from turbulent atmosphere to water waves, J. Oceanogr. Soc., Japan, 30, 97-107

HASSELMANN,K. et al. (1973): Measurements of wind-wave growth and swell decay during the Joint North Sea Wave Project (JONSWAP),

Ergänzungsheft zur Dt. Hydro. Z , Reihe A, 12, 1-95.

ICHIKAWA,H. and N.IMASATO (1976): The wind field over wind-waves, J. Oceanogr. Soc., Japan (in press)

IMASATO,N. (1976): Some characteristics on the development process of the wind-wave spectrum, J. Oceanogr Soc. Japan, 32, 21-32.

JEFFREYS,H. (1924): On the formation of waves by wind, Proc. Roy Soc. A, 107, 189-206.

KAKINUMA,T., A.ISHIDA and T.MONJI (1968): Analysis of nonlinearity of coastal ocean waves, Proc. 15th Conf. on Coastal Engn. in Japan, 73-79 (in Japanese).

KINSMAN,B. (1965): Wind waves, Prentice-Hall, Inc., New Jersey, 587-636.

KUNISHI,H. (1963): An experimental study on the generation and growth of wind waves, Bull, Disast. Prev. Res. Inst., Kyoto Univ., 61, 1-41.

LIGHTHILL,M.J. (1962): Physical interpretation of the mathematical theory of wave generation by wind, J. Fluid Mech., 14, 385-398.

MILES,J.W. (1957): On the generation of surface waves by shear flows, J. Fluid Mech., 3, 185-204.

MILES,J.W. (1959): On the generation of surface waves by shear flows. Part 2, J. Fluid Mech., 6, 568-582.

MILES,J.W. (1960): On the generation of surface waves by turbulent shear flows, J. Fluid Mech., 7, 469-478.

MILES,J.W. (1962a): On the generation of surface waves by shear flows. Part 4, J. Fluid Mech., 13, 433-448.

MILES,J.W. (1962b): A note on the inviscid Orr-Sommerfeld Equation, J. Fluid Mech., 13, 427-432

MITSUYASU,H. (1968): On the growth of the spectrum of wind-generated waves (I), Report, Res Inst. Appl. Mech., Kyushu Univ., XVI, 55, 459-482.

NAGATA,Y. (1970): Lag joint probability, higher order covariance function and higher order spectrum, La mer, 8, 78-94.

PHILLIPS, O.M. (1957): On the generation of waves by turbulent wind, J Fluid Mech., 2, 417-445.

PHILLIPS,O.M. (1958): The equilibrium range in the spectrum of wind-generated waves, J. Fluid Mech., 4, 426-434.

PHILLIPS,O.M. (1966): The dynamics of the upper ocean, Combridge Univ. Press, London, 87-101.

REYNOLDS,W.C. and F.HUSSAIN (1972): The mechanics of an organized wave in turbulent shear flow, Part 3., J. Fluid Mech., 54, 263-288.

SCHLICHTING,H. (1955): Boundary layer theory, McGraw-Hill, 4th Ed.,522-52

SHEMDIN,O.H. and E.Y.HSU (1967): Direct measurement of aerodynamic pressure above a simple progressive gravity wave, J. Fluid Mech., 30, 403-416.

SNYDER,R.L. and C.S.COX (1966): A field study of the wind generation of ocean waves, J Mar Res., 24, 141-178.

YEFIMOV,V.V. (1970): On the structure of the wind velocity field in the atmospheric near-water layer and the transfer of wind energy to sea waves, Izv Atmos. Oceanic Physics, 6, 1043-1053.

TUKEY,J.W (1963): What can data analysis and statistics offer today?, Ocean Wave Spectra, 347-351.

	RUN NO.	τ_{ws}	δf (Hz)	$\frac{\delta f}{f_R}$
Ex-K	11	1.249×10^{-5}	11.83*	1.000
F=12.4m	12	6.209×10^{-4}	11.50*	1.000
	13	7.432×10^{-3}	1.59	0.0993
	14	3.650×10^{-2}	0.876	0.0620
	15	7.955×10^{-2}	0.611	0.0509
	16	1.147×10^{-1}	0.314	0.0269
	17	1.843×10^{-1}	0.279	0.0245
	18	2.393×10^{-1}	0.306	0.0280
	19	3.916×10^{-1}	0.257	0.0228
	20	1.339	0.176	0.0153
Ex-K	11	4.932×10^{-6}	11.17*	1.000
F= 7.1m	12	3.260×10^{-5}	11.50*	1.000
	13	1.423×10^{-3}	12.20*	1.000
	14	1.362×10^{-2}	0.603	0.0483
	15	2.751×10^{-2}	0.606	0.0460
	16	6.548×10^{-2}	0.306	0.0278
	17	8.152×10^{-2}	0.179	0.0174
	18	1.237×10^{-1}	0.105	0.0099
	19	2.142×10^{-1}	0.123	0.0111
	20	5.885×10^{-1}	0.087	0.0078
Ex-KI	51	3.843×10^{-1}	0.100	0.0109
F=16.8m	52	9.711×10^{-1}	0.093	0.0099
	54	1.944	0.079	0.0082 †
	56	3.384	0.060	0.0062 †
	60	4.758	0.027	0.0028 †
	62	6.414	0.024	0.0025 †

Table 1(a); τ_{ws}, δf and $\delta f/f_R$ obtained from the wind tunnel experiments. Asterisk (*) indicates the relation $\delta f = f_R$.

DATE	TIME	τ_{ws}	δf (Hz)	$\frac{\delta f}{f_R}$
	h m h m			
1968-06-09	13 50-13 55	2.182×10^{-1}	1.55*	1.000
	13 55-13 59	9.874×10^{-2}	0.850	0.300
	14 37-14 43	9.446×10^{-2}	1.050*	1.000
1968-06-10	9 53- 9 59	3.920×10^{-2}	0.667	0.235
	12 07-12 17	3.204×10^{-2}	0.350	0.128
	12 17-12 21	2.267×10^{-2}	0.300	0.112
1969-06-04	11 52-12 04	1.032×10^{-2}	0.600	0.129
1969-06-05	10 30-10 35	3.509×10^{-3}	3.100*	1.000
	10 35-10 48	4.476×10^{-3}	3.700*	1.000
	10 48-10 57	5.663×10^{-3}	3.000*	1.000
	10 57-11 03	7.704×10^{-3}	1.90	0.481
1969-06-06	11 34-11 48	1.531×10^{-2}	0.267	0.099
	11 48-11 52	2.031×10^{-2}	0.333	0.123
1969-06-07	6 13- 6 23	6.480×10^{-3}	0.400	0.133
1969-06-08	6 53- 6 56	3.688×10^{-2}	1.733	0.692

Table 1(b); τ_{ws}, δf and $\delta f/f_R$ obtained from the field observations at Lake Biwa. Asterisk (*) indicates the relation $\delta f = f_R$.

RUN NO.	FETCH (m)	E	τ_{ws}	δf (Hz)	$\frac{\delta f}{f_R}$
11	12.4	4.49	1.249×10^{-5}	4.00	0.501
12	12.4	2.72	6.209×10^{-4}	4.00	0.523
11	7.1	4.90	4.932×10^{-6}	3.00	0.500
12	7.1	4.21	3.260×10^{-5}	2.67	0.381
13	7.1	0.86	1.423×10^{-3}	4.00	0.462

Table 2; δf and $\delta f/f_R$ according to the MILES' (1962a) viscous model.

RUN NO.	FETCH (m)	f_{TS} (Hz)	f_{max} (Hz)
11	4.3	0.146	4.667
11	9.7	0.625	4.667
11	15.1	0.792	5.667

Table 3; The frequency f_{TS} giving the resonance between the TOLLMIEN-SCHLICHTING wave and the surface wind-waves.

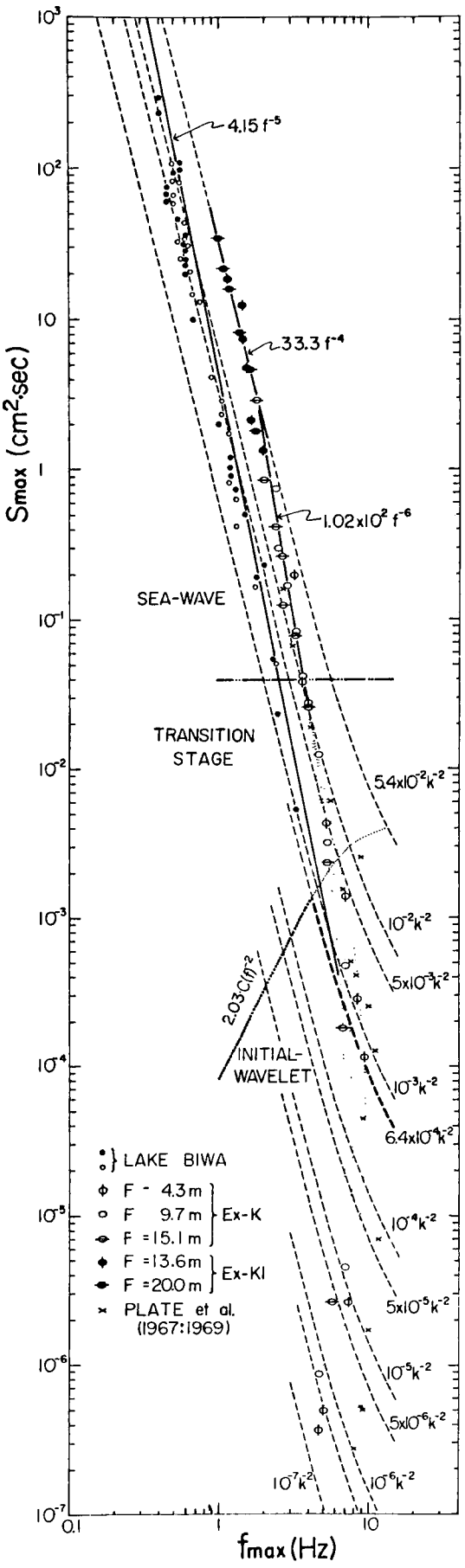

Figure 1; Development of wave spectral peaks. The solid line shows the line $4.15f^{-5}$ obtained from the field observations at Lake Biwa, and the broken curves show the wave spectra given by the equation 1 with some

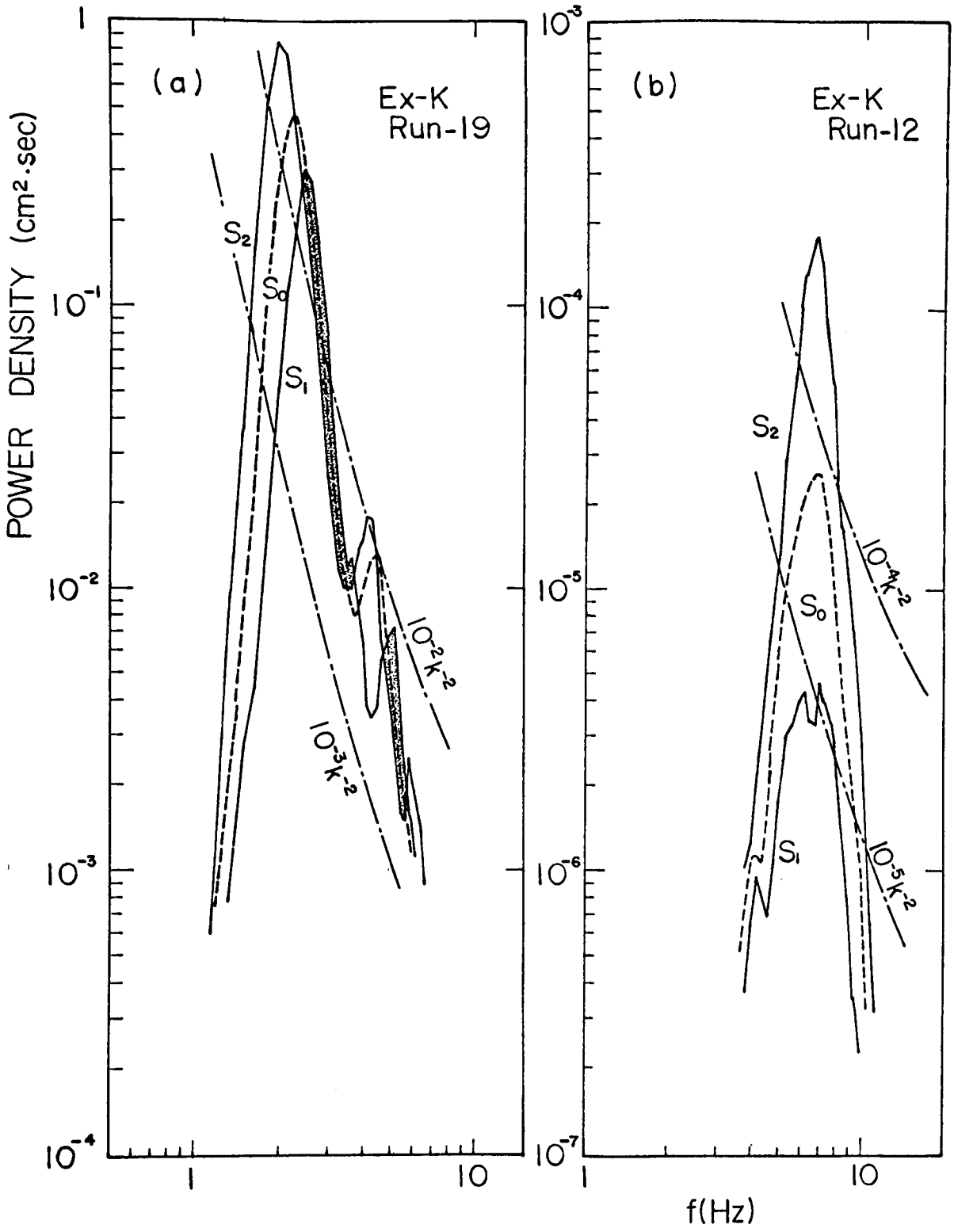

Figure 2; Schematic diagram of development of the wave spectrum; (a) is for wind-waves in the stage of "sea-waves" and (b) for those in the stage of "initial-wavelets". The wave spectrum $S_o(f)$ is estimated from the observed spectra $S_1(f)$ and $S_2(f)$. Chain curves show the wave spectra $S(f)=\alpha_1 k^{-2}$ with some values of α_1.

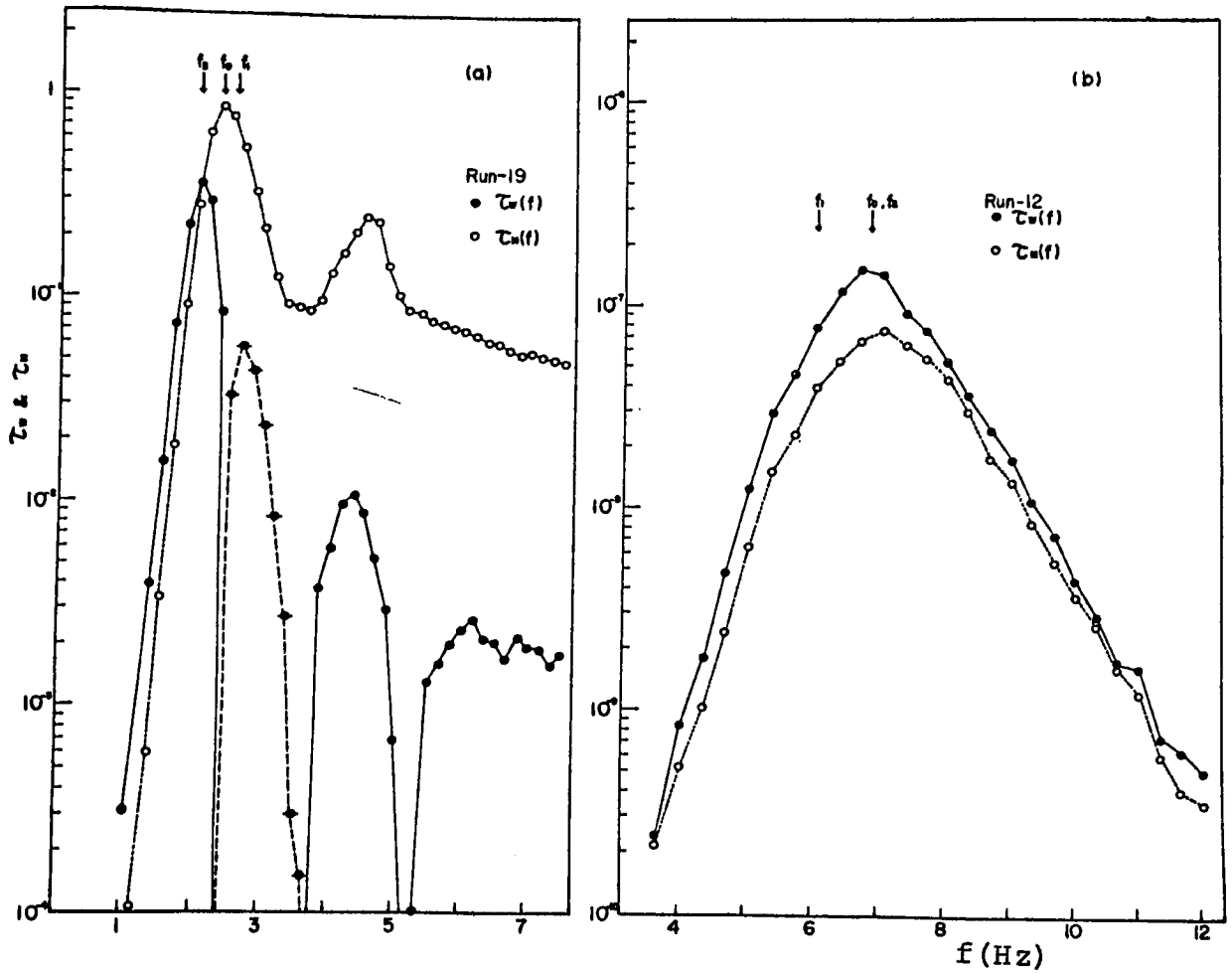

Figure 3 : The spectra of $\tau_M(f)$ (dotted curves) according to the MILES' inviscid model and $\tau_W(f)$ (solid curves); (a) is for the wind-waves in the stage of "sea-waves" and (b) for those in the stage of "initial-wavelets". The part, given by the mark -●- and the broken curve, shows the absolute value of negative part of $\tau_W(f)$. Arrows show the frequency f_{max} of wave spectral peaks.

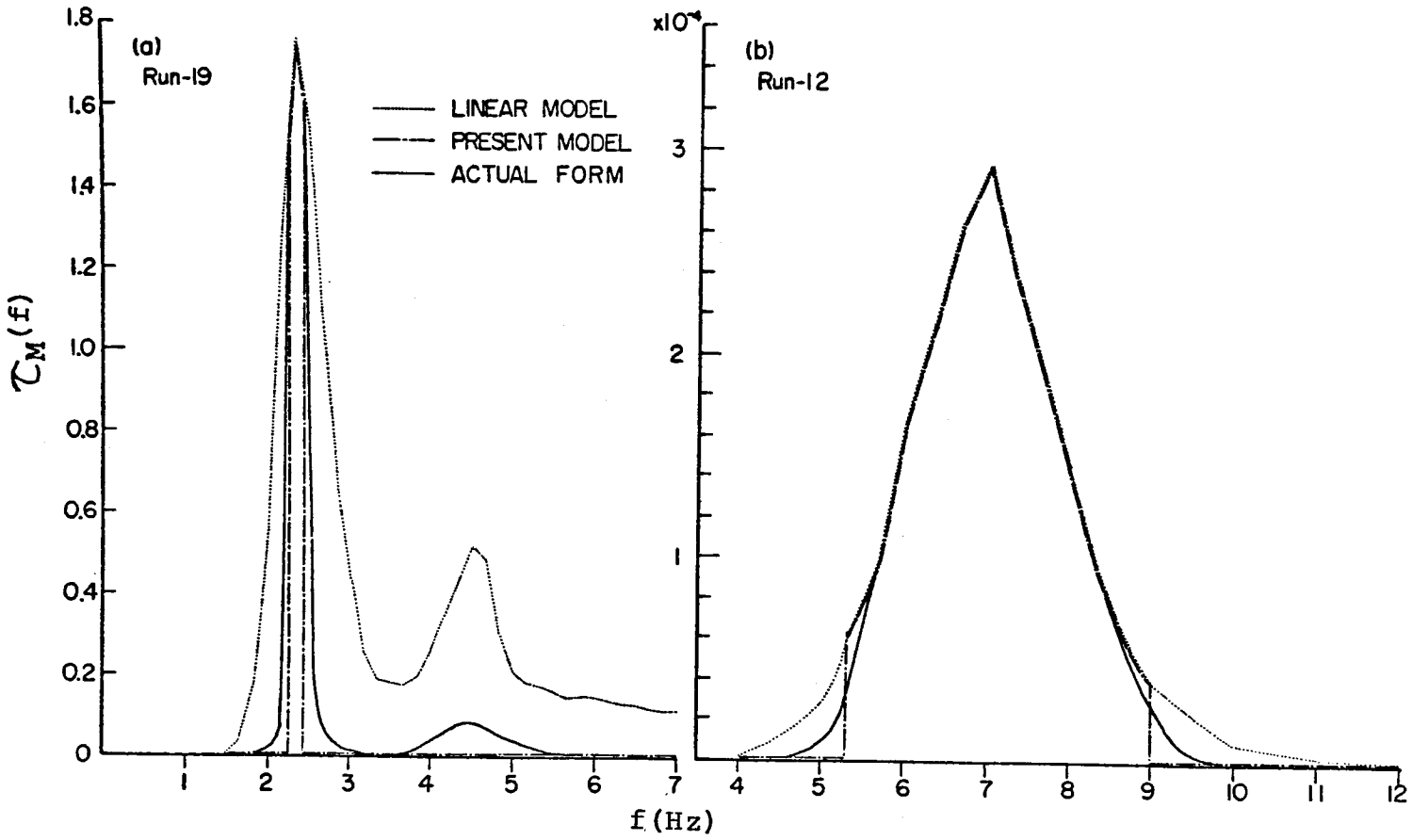

Figure 4; The momentum transfer filter. The dotted curve shows the calculated spectrum $\tau_M(f)$ according to the linear model after MILES (1960). The chain curve shows the spectrum $\tau_M(f)$ according to the present model, and the solid curve shows the actual form of the spectrum $\tau_M(f)$. (a) is for the wind-waves in the stage of "sea-waves" and (b) for those in the stage of "initial-wavelets."

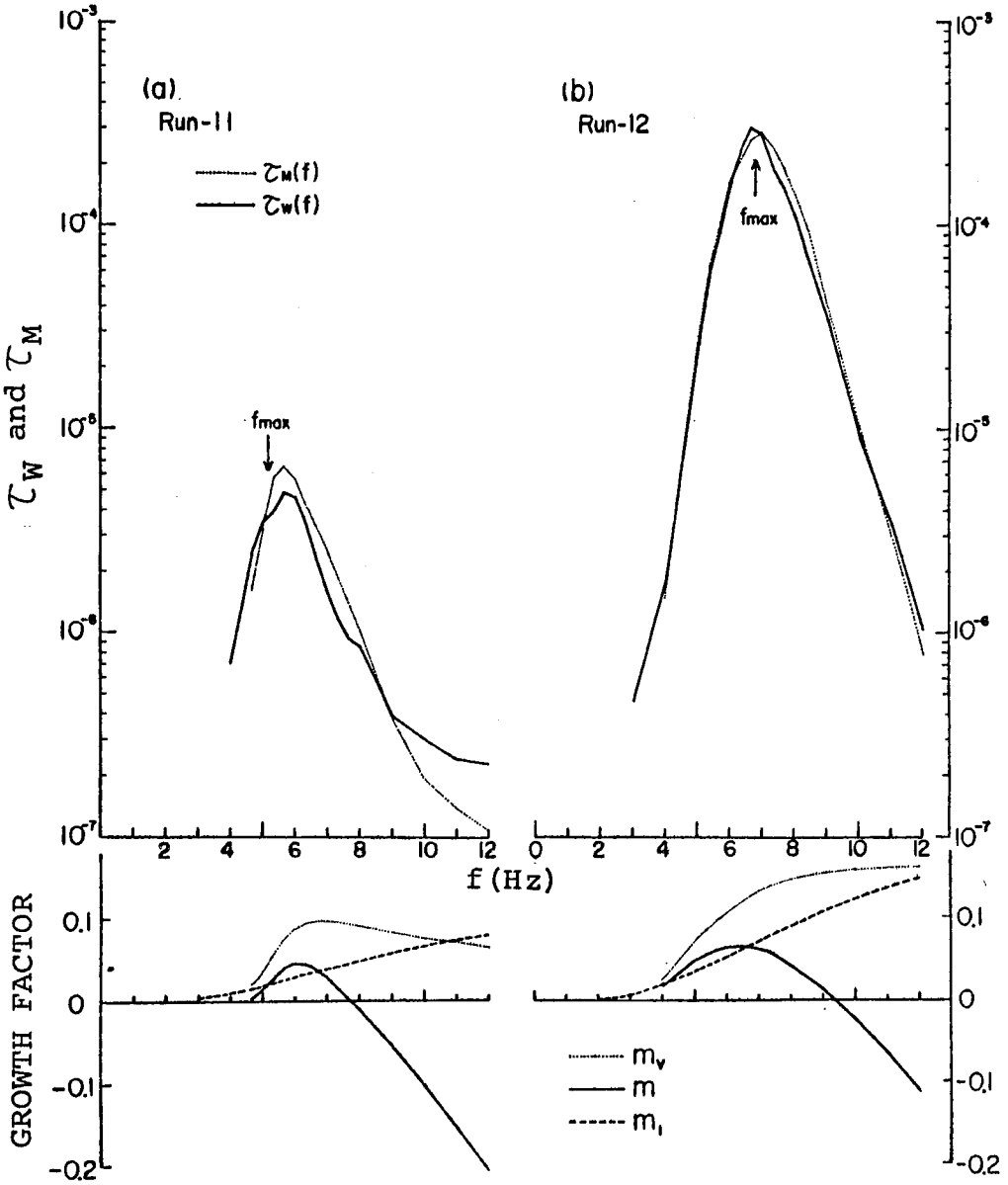

Figure 5; The upper part shows the spectra of $\tau_M(f)$ (dotted curves) according to the MILES' (1962a) viscous model and $\tau_w(f)$ (solid curves). The lower part shows the spectra of the growth rate of the "initial-wavelets". The dotted curves show the spectra $m_v(f)$ and the solid curves show the spectra m(f) according to the MILES' viscous model. The broken curves show the spectra $m_I(f)$ according to the MILES' (1960) inviscid model on the assumption of the logarithmic wind profile. They are evaluated at the fetch F=12.4m. (a) is for Run-11 and (b) is for Run-12 in the wind tunnel experiment Ex-K.

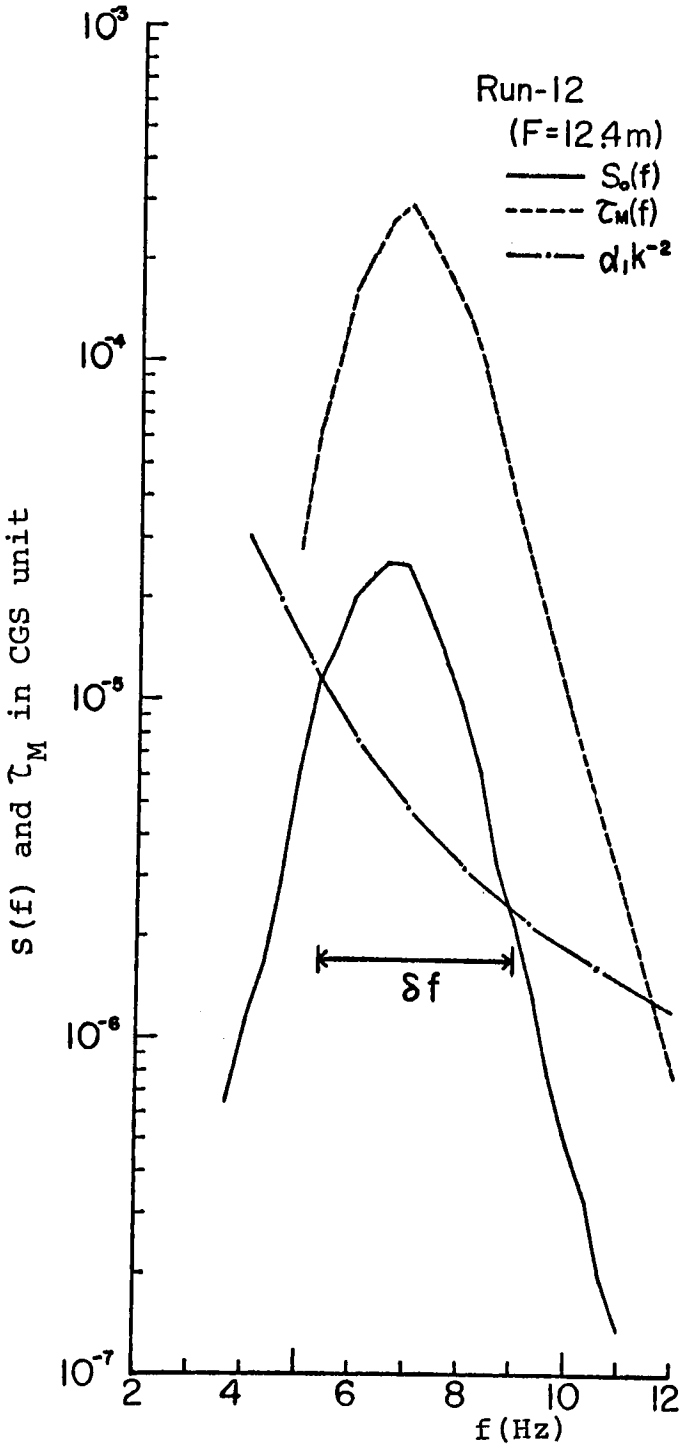

Figure 6; Schematic diagram showing the relation among $S_o(f)$ (solid curve), $\alpha_1 k^{-2}$ (chain curve) given by Eq.1, $\tau_M(f)$ (broken curve) and the frequency region δf.

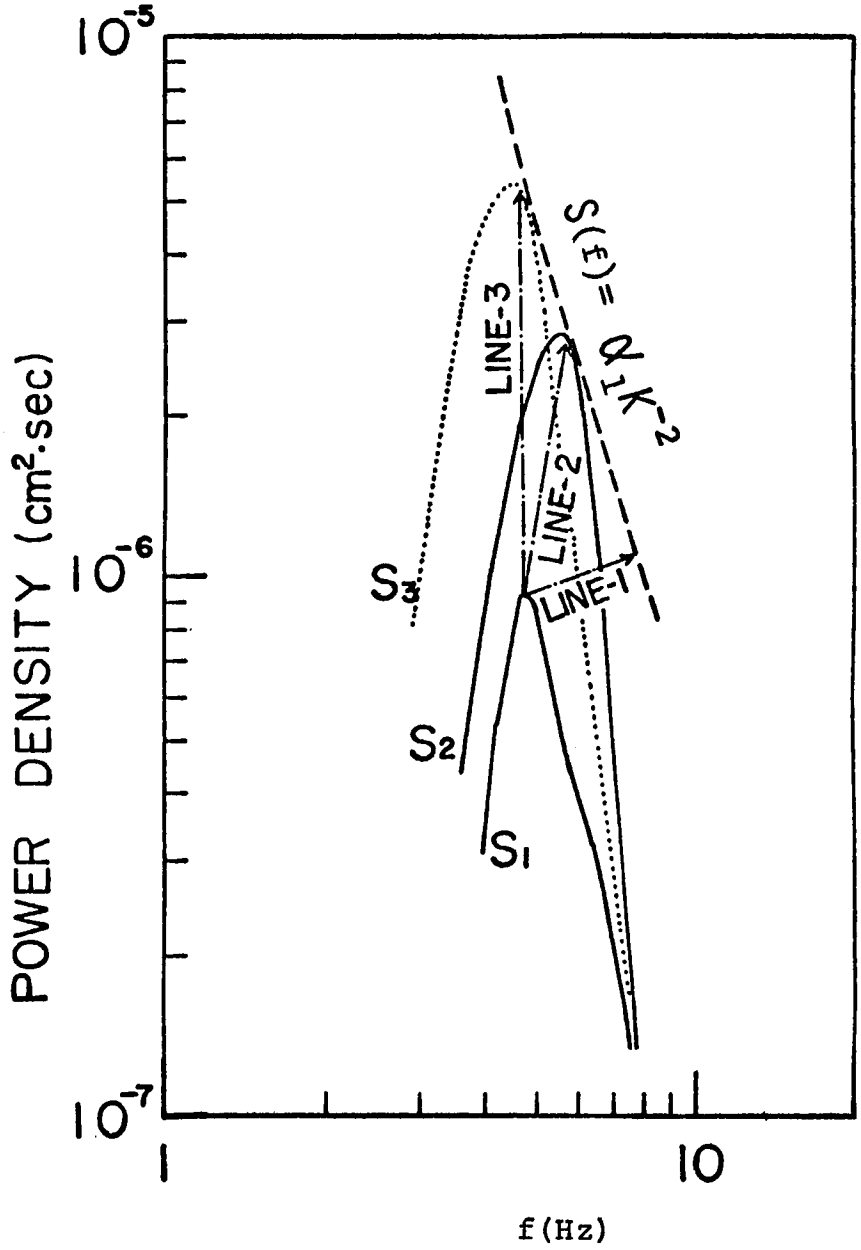

Figure 7; Schematic diagram explaining development process of the wave spectrum in the stage of initial-wavelets.

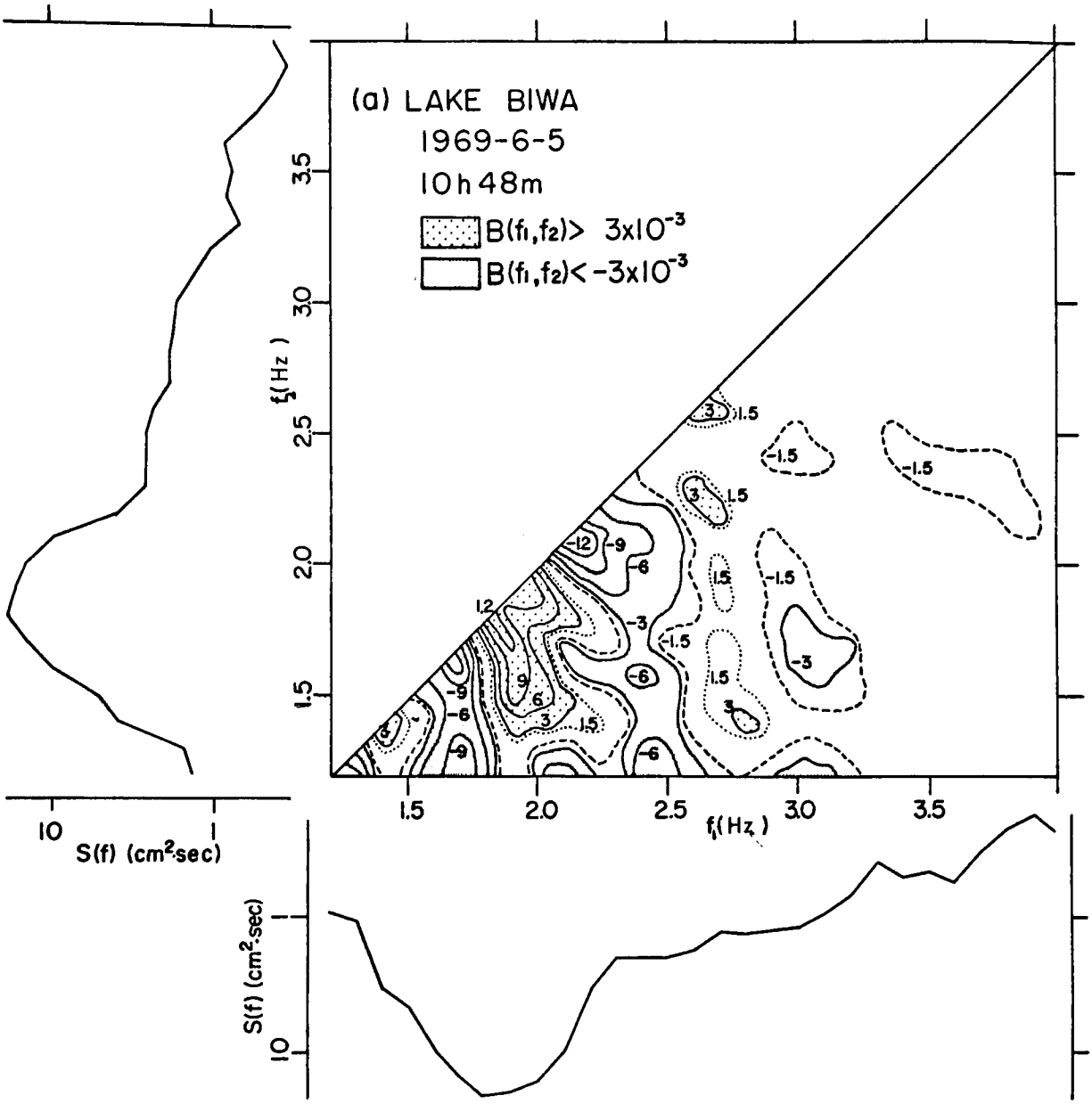

Figure 8(a); Bispectrum of wind-waves in the case of IS-06 obtained at Lake Biwa. The unit of contour curves of the bispectral density is $10^{-3}cm^3 \cdot sec^2$.

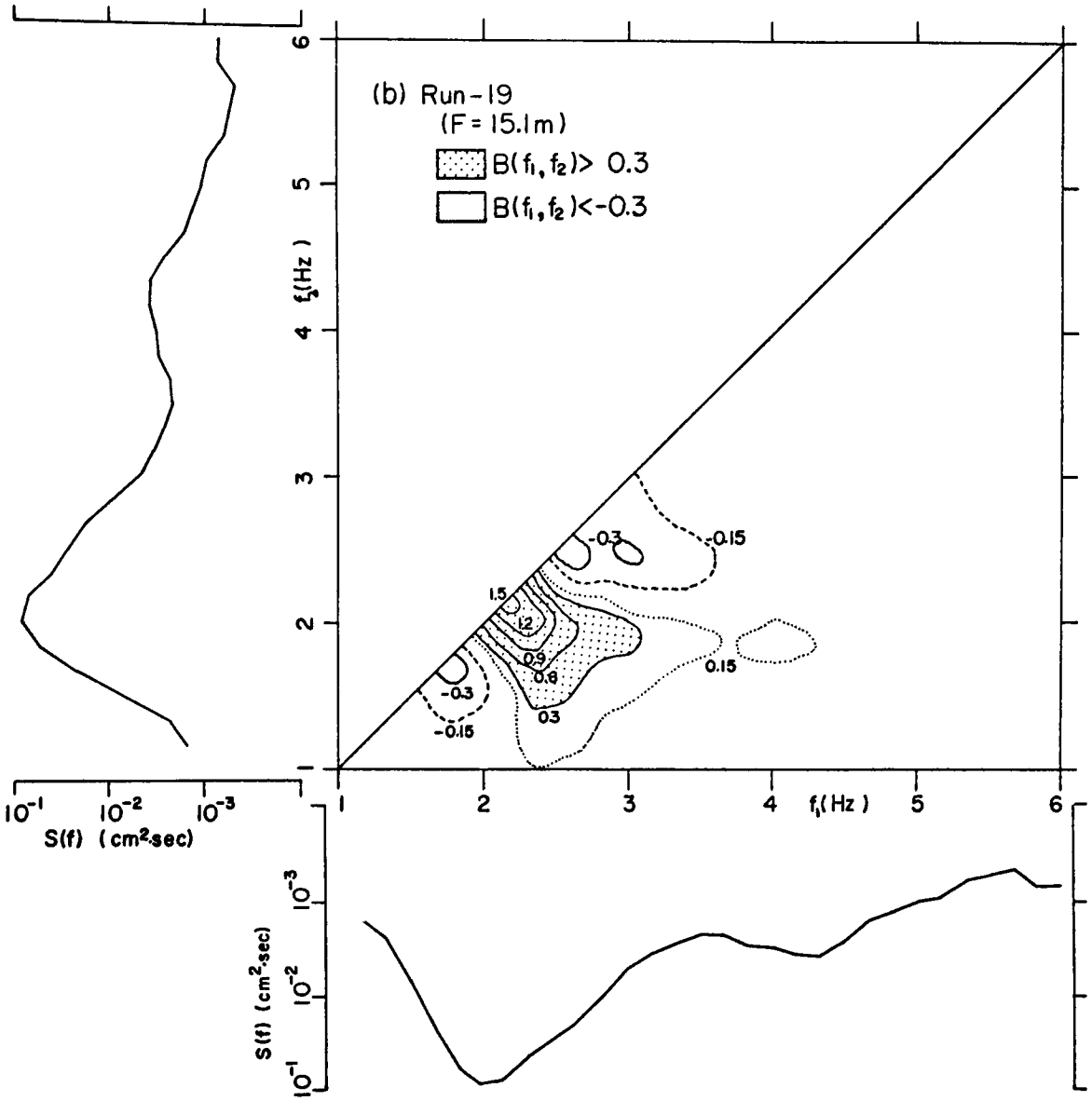

Figure 8 (b); Bispectrum of wind-waves in the stage of "sea-waves" in the wind tunnel. The unit of contour curves of the bispectral density is $1.0 cm^3 . sec^2$.

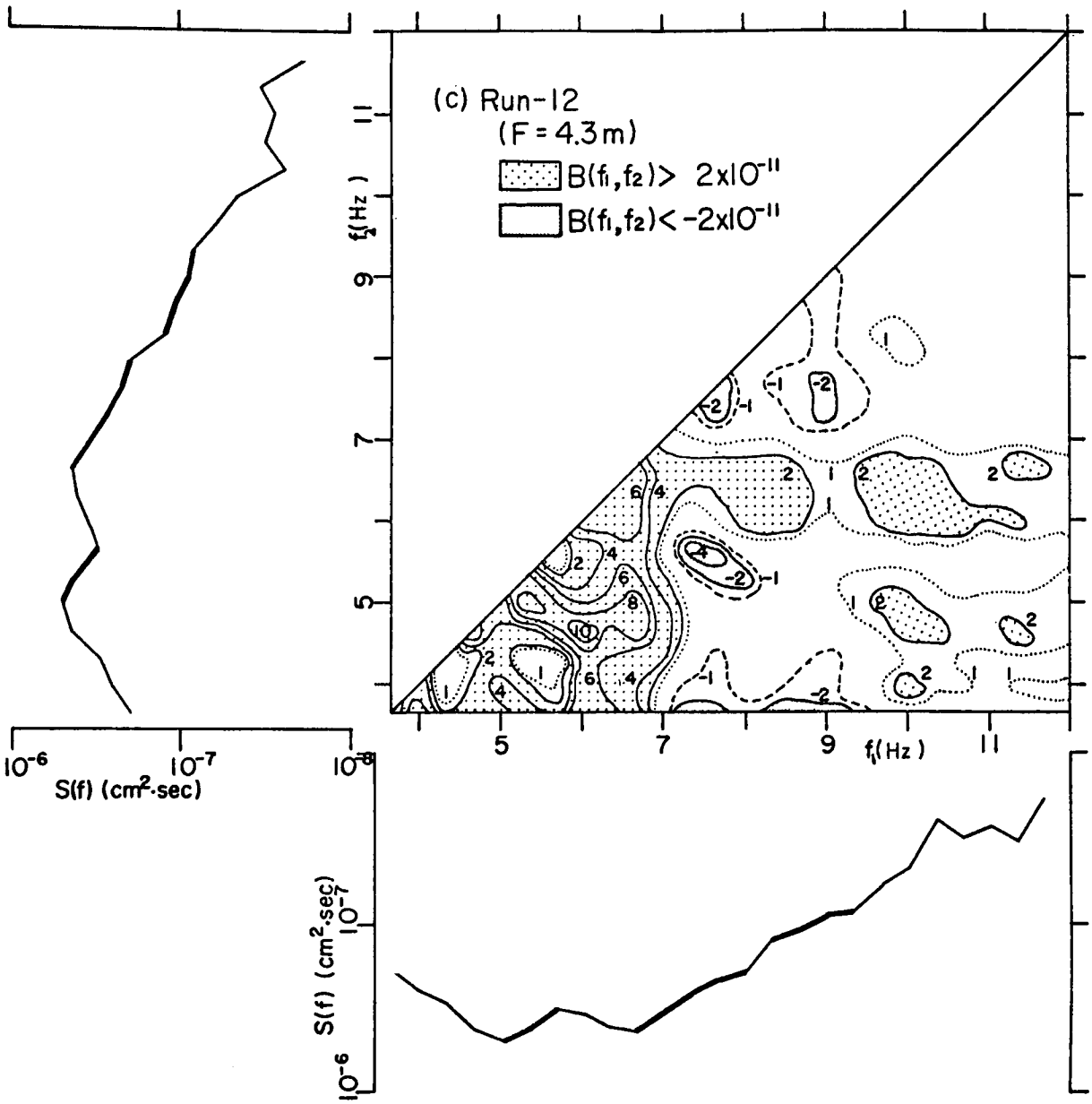

Figure 8(c); Bispectrum of wind-waves in the stage of "initial-wavelets" in the wind tunnel. The unit of contour curves of the bispectral density is 10^{-11} $cm^3 \cdot sec^2$.